ICARUS 107, 255–268 (1994)

Velocity Distributions among Colliding Asteroids

WILLIAM F. BOTTKE, JR., MICHAEL C. NOLAN, RICHARD GREENBERG, AND ROBERT A. KOLVOORD

Lunar and Planetary Laboratory, University of Arizona, Tucson, Arizona 85721
E-mail: bottke@lpl.arizona.edu

Received August 9, 1993; revised November 15, 1993

The probability distribution for impact velocities between two given asteroids is wide, non-Gaussian, and often contains spikes according to our new method of analysis in which each possible orbital geometry for collision is weighted according to its probability. An average value would give a good representation only if the distribution were smooth and narrow. Therefore, the complete velocity distribution we obtain for various asteroid populations differs significantly from published histograms of average velocities. For all pairs among the 682 asteroids in the main-belt with $D > 50$ km, we find that our computed velocity distribution is much wider than previously computed histograms of average velocities. In this case, the most probable impact velocity is ~4.4 km/sec, compared with the mean impact velocity of 5.3 km/sec. For cases of a single asteroid (e.g., Gaspra or Ida) relative to an impacting population, the distribution we find yields lower velocities than previously reported by others. The width of these velocity distributions implies that mean impact velocities must be used with caution when calculating asteroid collisional lifetimes or crater-size distributions. Since the most probable impact velocities are lower than the mean, disruption events may occur less frequently than previously estimated. However, this disruption rate may be balanced somewhat by an apparent increase in the frequency of high-velocity impacts between asteroids. These results have implications for issues such as asteroidal disruption rates, the amount/type of impact ejecta available for meteoritical delivery to the Earth, and the geology and evolution of specific asteroids like Gaspra.

I. INTRODUCTION

Collisions determine the history of asteroids, affecting cratering of surfaces, development of regolith, and controlling lifetimes to disruption. Most models of asteroid collisions take into account the distribution of masses of other impacting asteroids, since impactor size is important to understanding the significance of various collision events. However, those models generally assume that the distribution of collision velocities is sufficiently narrow that it can be represented by a single representative average velocity. For the main asteroid belt, $\langle V \rangle$ is generally taken to be 5 km/sec. Asteroid collisional modeling has now reached a level of sophistication where velocity distributions need to be considered, especially since collision effects are very sensitive to impact velocity (e.g., the impact kinetic energy goes as V^2).

The statistical mechanics of asteroid interactions has been usually based on "particle-in-a-box" models obtained from gas dynamics, where particles are assumed to travel at constant velocity between impacts. However, the statistical mechanics of Solar System bodies is significantly different from that of gas particles. An individual particle in a Keplerian orbit moves at an ever-changing velocity which is a function of its position. As we will show, for a given pair of asteroids, some impact velocities are much more probable than others.

Starting with Öpik (1951), models have been developed that more accurately compute the collision probabilities between a pair of bodies on Keplerian orbits. (Wetherill 1967, Greenberg 1982, Bottke and Greenberg 1993). These methods calculate collision probabilities between bodies with fixed semimajor axes, eccentricities, and inclinations, integrating over uniform distributions of longitudes of apsides and nodes to account for precession. These models more accurately represent the range of collision geometries between a pair of bodies than particle-in-a-box models can.

Applying the methods of Wetherill (1967), Namiki and Binzel (1991) and Farinella and Davis (1992) used the same integration ranges and geometry to obtain average velocities for representative populations impacting a target body. These models used a representative population that included the larger bodies in the main-belt, which they assumed to provide an orbital distribution characteristic of all main-belt asteroids. The velocities were computed by taking pairs of bodies (i.e., the target body and members of the representative population) and, for each pair, averaging over all of their possible collision geometries. Then they produced a histogram of average velocities over all pairs, which they displayed as a velocity distribution. The average of these velocity averages was taken as representative of collision velocities involving this population.

0019-1035/94 $6.00

That procedure has three limitations:

I.1. The average velocity computed for a given pair of bodies did not account for the relative probability of each possible collision geometry. Instead, they assumed each evaluated collision geometry was equally probable. Consequently, since their averaging process was not properly weighted, the average collision velocity obtained for each pair is not accurate.

I.2. The average collision velocity for a given pair of bodies, even if calculated correctly, may not be a good representation of the probability distribution of collision velocities if this distribution is highly non-Gaussian (which, as shown later, is the case).

I.3. The published velocity distributions representing results over many pairs of asteroids are actually histograms of the average velocities for each pair. Such distributions are not equivalent to the velocity probability distribution that is obtained by summing the separate probability distributions.

In this paper, we develop a method for determining velocity distributions and apply it to individual pairs of bodies. We add these individual distributions to obtain velocity distributions for sets of pairs of asteroids (e.g., the set of Gaspra and every other main-belt asteroid ($D > 30$ km)). These results are significantly different from the histograms of average velocities for these same populations computed by Namiki and Binzel (1991) and Farinella and Davis (1992). We also obtain distributions of the directional components of velocity for collisions in the main-belt and compare our results to those of Magnusson (1993). Finally, we discuss the applications of our work to understand the asteroid collisional record.

II. COLLISION PROBABILITIES AND VELOCITY DISTRIBUTIONS

II.A. Distribution for a Single Pair of Bodies

In order to find the collision probability and velocity distribution between pairs of bodies orbiting the Sun, we follow the formulation of the Öpik/Wetherill approach by Greenberg (1982) with corrections by Bottke and Greenberg (1993). This formulation avoids most singularities in the collision probability integral even for orientations between orbital pairs that involve orbital crossings near an apse of one orbit. This approach requires only the "fixed parameters" of the semimajor axis, eccentricity, and inclination (a, e, i) of each body as input and assumes that they will change little over time. The apsides and the nodes describing the orientation of each orbit are assumed to precess uniformly, ignoring effects of secular perturbations for two reasons: First, such perturbations force apsidal and nodal longitudes to precess through a cycle (and other elements to oscillate) on a much shorter time scale than that between asteroid collisions ($\sim 10^4$ vs $\sim 10^6$ years); second, the distribution of precession phases should be fairly uniform for large populations of asteroids. This assumption was tested by numerical integration experiments (Davis *et al.* 1992) and discussed by Farinella and Davis (1992), who found it to be reasonable in most cases. Specifically, they concluded:

II.1. Few asteroids have orbital elements that yield significant nonuniform precession of apsidal and nodal longitudes (Knezevic *et al.* 1991).

II.2. Secular perturbations can modify an asteroid's eccentricity and inclination (and therefore its collision probability and impact velocity), but that these variations are of secondary importance over long time scales, since minor fluctuations in a body's orbit are likely to average out. To minimize inaccuracies produced by osculating elements away from long-term average values. Farinella and Davis use the proper elements of Milani and Knezevic (1990).

II.3. A large representative sample of a population of bodies (in this case, the hundreds of asteroids in the main-belt with $D > 50$ km) tends to average away small orbital modifications. Consequently, osculating elements are expected to yield results similar to proper elements when large data sets are used.

The formulation denotes one body in each pair as a "field body" and one as a "test body," with orbital elements given by (a_0, e_0, i_0) or (a, e, i), respectively. With the assumption that the arguments of pericenter (ω and ω_0) and the difference between the longitudes of ascending node ($\Omega - \Omega_0 \equiv \Delta\Omega$) vary uniformly with time, we calculate the collision velocities at each possible collision orientation. Weighting those velocities by the collision probability per time P_G at each orientation, we obtain the mean collision velocity for a pair of bodies,

$$\langle V \rangle = \frac{\int_0^{2\pi} \int_{\omega_0} P_G(\omega_0, \Delta\Omega) V(\omega_0, \Delta\Omega) d\omega_0 d(\Delta\Omega)}{\int_0^{2\pi} \int_{\omega_0} P_G(\omega_0, \Delta\Omega) d\omega_0 d(\Delta\Omega)}, \quad (1)$$

with

$$P_G = \frac{4}{(2\pi)^3} \left(\frac{\tau f}{\sin(u - \omega)} \right) \left(\frac{\pi P_0}{4T} \right) \left(\frac{1}{\tau^2} \right). \quad (2)$$

τ is the radius of the collision cross section, u is the distance of the orbital intersection from the test body's node, P_0 is the probability of impact for precisely intersecting orbits at this geometrical site, T is the orbital period of the test body, and f is a function of orbital elements, all as defined by Greenberg (1982). Note that the denominator in (1) is the intrinsic collision probability (P_i) as defined by Wetherill. Although P_G depends on ω

as well as ω_0 and $\Delta\Omega$, at an orbital intersection ω is a function of the other orbital elements, so we only need to integrate over ω_0 and $\Delta\Omega$ in (1).

As noted in the Introduction (Point I.1), neither Namiki and Binzel (1991) nor Farinella and Davis (1992) weighted the collision velocity at each orientation by the collision probability. In effect, for a given pair of orbits, all possible collision encounter geometries (steps in ω_0 and $\Delta\Omega$) were treated as equally probable, making all collision velocities equally weighted, as if P_G were constant in (1). However, P_G is, in fact, highly variable, e.g., collisions near an apse of one orbit are much more probable than other particular orientations. An accurate computation requires that this weighting function be included in the calculation.

We estimate the size of the difference created by collision velocity weighting (Point I.1) by comparing average collision velocities found using the method of Namiki and Binzel (1991) and Farinella and Davis (1992) with those found using Eq. (1). To test the Namiki and Binzel (1991) algorithm, we computed the average velocities between various objects with the hypothetical asteroid "Astrid" (objects described in Bottke and Greenberg (1993)). The results showed that their algorithm yielded average collision velocity values ~0.3–1.5 km/sec lower than those of Eq. (1). Though we were unable to test the Farinella and Davis (1992) algorithm for the same data set, we were able to compare Eq. (1) with their average collision velocity results for selected main-belt asteroids with the population of 682 main-belt asteroids (their Table 1). For this data set, the results showed that their algorithm yielded average collision velocities values ~0.2–0.7 km/sec higher than those of Eq. (1). We conclude that proper weighting of collision geometries is very important.

If a single velocity value (e.g., the average given by Eq. (1)) is used to represent any encounter between a pair of asteroids, the true velocity distribution is in effect being represented by a spike. Thus, even when the average velocity is obtained with appropriate weighting, as in (1), it may not be a good representation of the distribution of velocities if that distribution is wide, skewed, or spiky. In such cases, only the actual probability distribution of velocities provides adequate treatment of the possible collision velocities (Point I.2).

Obtaining the complete velocity probability distribution for a pair of orbits requires an additional process beyond the evaluation of Eq. (1). The numerical integration required to evaluate Eq. (1) involves computing the impact velocity V and the probability P_G in many small increments ($\Delta\omega_0\Delta(\Delta\Omega)$). To get the velocity distribution, we divide the full range of possible values of V into small bins of width ΔV. Then, during the numerical integration of Eq. (1), we keep a running total of the values of $P_G(\omega_0, \Delta\Omega)\Delta\omega_0\Delta(\Delta\Omega)$ that correspond to the values of V within each ΔV bin. In this way we build up the probability histogram for impact velocities for this given pair of orbits. The total area under this velocity distribution is the intrinsic collision probability. For the velocity distributions shown in this paper, we have integrated (1) with Gaussian quadrature techniques (Press *et al.* 1986) and simultaneously built up the velocity histogram using (at least) 100,000 evaluation points for each orbital pair. Experiments with narrower stepsizes (more points) showed no significant change in results.

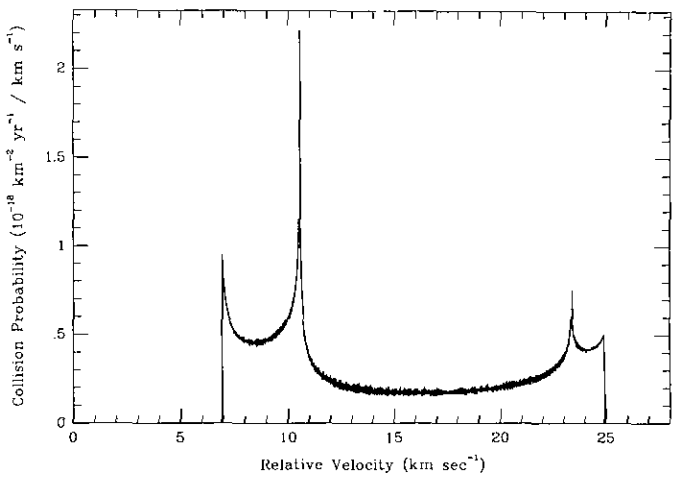

FIG. 1. Velocity distribution between two hypothetical asteroids. The test asteroid (a = 3.42, e = 0.578, i = 0.435 rad) crosses the field body's orbit (a_0 = 1.59, e_0 = 0.056, i_0 = 0.466 rad). Note that no averaged velocity adequately represent this distribution. These peaks are characteristic of encounters near the apse of one body's orbit, where there is a wide range of collision orientations that give the same (usually extreme) collision velocity.

We find that the shapes of these distributions are generally non-Gaussian and often include spikes. Such distributions are not well characterized by any single average velocity (Point I.2). The most likely collision velocities are often near the low and high velocity extremes. An example of a velocity distribution between two hypothetical bodies is shown in Fig. 1. In this case, the test body, in an eccentric and inclined orbit (a = 3.42, e = 0.578, i = 0.435 rad), crosses the more circular similarly inclined field body's orbit (a_0 = 1.59, e_0 = 0.056, i_0 = 0.466 rad). The mean collision velocity $\langle V \rangle$ falls in the low-probability valley between the high-probability peaks near each velocity extreme. These peaks are characteristic of encounters near the apse of one body's orbit, where there is a wide range of collision orientations that give the same (usually extreme) collision velocity. The result shown in Fig. 1 is typical of velocity distributions seen for other pairs of bodies. Thus, the mean velocity is not a meaningful representation of this distribution, confirming Point I.2.

II.B. Collision Velocities among Populations of Bodies

The velocity distribution of a population of asteroids is obtained by summing the velocity distributions of all possible pairs in the population. Because each pair has a spiky distribution (e.g., Fig. 1) the sum of these individual velocity distributions can be full of spikes and fine structure. However, for large enough populations, most individual spikes are smoothed out, and generally the distributions is more nearly Gaussian. Even so, the distributions are wide and complex enough that no single characteristic velocity value adequately describes them.

A different approach was taken by Namiki and Binzel (1991) and by Farinella and Davis (1992) to obtain velocity distributions for entire populations (see Introduction). Rather than add velocity distributions for every pair in a population, they produced a histogram displaying the average velocities for each pair and interpreted this as the velocity distribution for a target object with an impacting population. However, as noted in Point I.3, each average velocity does not fully represent the velocity distribution for a given pair. For example, suppose each pair of asteroids had a very wide distribution of velocities, but all average velocities were nearly the same. The approach of Namiki and Binzel or Farinella and Davis would give a narrow range of velocities for the whole population, when in fact, the actual distribution of velocities would be very wide.

III. RESULTS

The sets of orbits used in our calculation are assumed to be representative of entire asteroid populations, even though they are the orbits for only a sample of that population. In this regard, we are following an assumption by Namiki and Binzel (1991) and Farinella and Davis (1992). For the main asteroid belt, we avoid observational bias by setting size limitations on the asteroid sample. Namiki and Binzel assumed that nearly all of the larger asteroids with diameters ($D > 30$ km) have been discovered, so this set of asteroids is a non-observationally biased sample of a representative orbital distribution. We use the same set of asteroids and osculating orbital elements (calculated by the Minor Planet Center) in our calculations to allow direct comparison of our results with those obtained by Namiki and Binzel (1991). However, Farinella and Davis investigated a sample of 682 asteroids with diameters $D > 50$ km, because they believed that taking a minimum diameter at 30 km could introduce a bias against dark, outer-belt objects which may not be complete down to 30 km (Cellino *et al.* 1991); for comparison with their work we use the same set of asteroids and orbital elements (from Milani and Knezevic 1990) as they did.

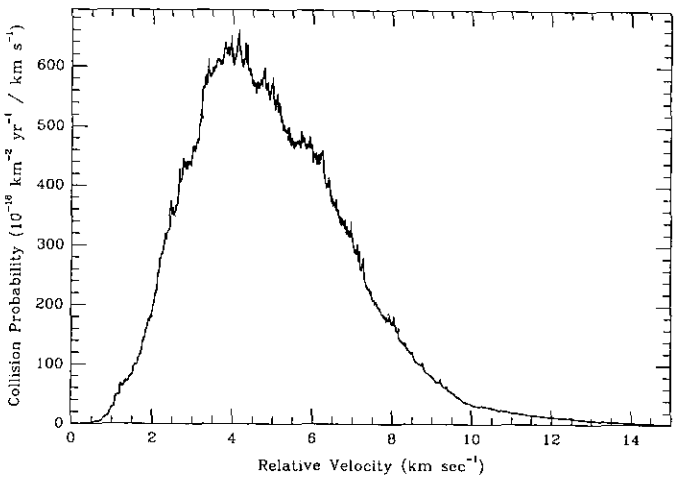

FIG. 2. Velocity distribution for the 533 main-belt asteroids of diameter >30 km whose orbits intersect 951 Gaspra. The mean, median, and rms collision velocities are 5.02, 4.76, and 5.41 km/sec, respectively. Note that the area under the curve, divided by the number of orbital crossing pairs, is the mean intrinsic collision probability: $\langle P_i \rangle_{CROSS} = 5.53 \times 10^{-18}$ km^{-2} year^{-1}. The spiky features are real, not noise, representing the collision distributions of actual pairs of asteroids.

III.A. Velocity Distributions for Selected Asteroids

III.A.1. 951 Gaspra. Asteroid 951 Gaspra intersects the orbits of 533 asteroids with $D > 30$ km as of April 1993 (according to Minor Planet Center osculating elements). Figure 2 shows the velocity distribution for all possible collisions, i.e., the sum over 533 pairs (Gaspra and all other crossers). The distribution is quasi-Gaussian but spiky, with the spikiness a consequence of Gaspra's high collision probability over particular collision geometries with individual asteroids. Its mean intrinsic collision probability for those particular crossing asteroids is $\langle P_i \rangle_{CROSS} = 5.53 \times 10^{-18}$ km^{-2} year^{-1}, while the mean collision velocity is $\langle V \rangle = 5.0$ km/sec. However, the distribution is sufficiently wide and complex that no single average collision velocity adequately describes it. The mean is much greater than the most probable collision velocities (~3.6 to 4.4 km/sec), a consequence of the long high-velocity tail (similar to a Gaussian distribution). Roughly 10% of Gaspra impactors hit at velocities $V >$ 8 km/sec, twice as large as the most probable impact velocities. These higher impact velocities stem from encounters with main-belt asteroids with high eccentricities and inclinations.

The area under the velocity distribution histogram represents the total intrinsic collision probability for all crossing pairs. In order to obtain the average intrinsic collision probability for the crossing bodies ($\langle P_i \rangle_{CROSS}$), one divides this area by the number of crossing bodies ($N_{CROSS} = 533$). However, Farinella and Davis (1992) noted that one can obtain the collision probability averaged over a larger

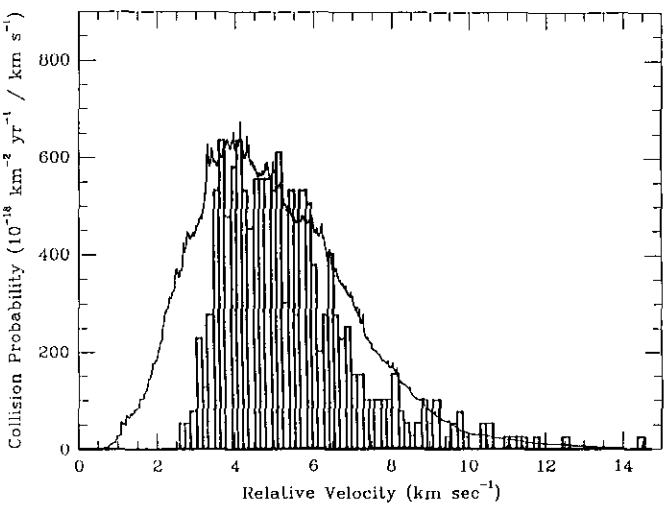

FIG. 3. Histogram of average velocities $\langle V \rangle$ for the same population in Fig. 2 superimposed on Fig. 2, from Namiki and Binzel (1991). A comparison between this histogram and the velocity distribution from Fig. 2 shows that the histogram of average velocities misses low collision velocities and some of the velocity structure present in the actual velocity distribution.

base population that includes some fraction of noncrossers (e.g., all main-belt asteroids over 30 km) by dividing the area under the velocity distribution histogram by the number of bodies in the population. Gaspra's collision probability relative to the entire main-belt population (1052 asteroids with $D > 30$ km) is

$$\langle P_i \rangle_{POP} = \langle P_i \rangle_{CROSS} \left(\frac{533}{1052} \right) = 2.80 \times 10^{-18}\,\mathrm{km}^{-2}\,\mathrm{year}^{-1}.$$

We compare Gaspra's velocity distribution with the distribution published by Namiki and Binzel (1991) (Fig. 3), which was actually a histogram of average velocities. (We used updated orbital elements for Gaspra and Ida crossers, slightly different from those used by Namiki and Binzel, but the effect is negligible.) We find a significant probability (~15%) of impact below 3 km/sec, which did not appear in their results. Furthermore, the fine structure seen in our distribution is due to possible apsidal encounters among individual pairs. In contrast, the histogram of average velocities has spikes and gaps that are a consequence of the discreteness of the Namiki and Binzel method and are not real (Binzel, personal communication). Finally, we find a distinct difference between their reported root mean square velocity (5.0 km/sec) and our rms velocity (5.41 km/sec), which results from the improvements intrinsic to our method. The effects of these collision probabilities and velocities on Gaspra's lifetime against catastrophic disruption will be discussed further in Section IV.

We can also compare the velocity distribution for Gaspra impactors with results by Farinella *et al.* (1991). For a valid comparison, we use the same population as they did (asteroids with $D > 50$ km) and the same set of proper orbital elements. Farinella and Davis reported values an average collision velocity of 5.45 km/sec and a $\langle P_i \rangle_{POP}$ of $2.69 \times 10^{-18}\,\mathrm{km}^{-2}\,\mathrm{year}^{-1}$ (although their distribution was not published). For this population we obtain a velocity distribution very similar to what we found in Fig. 2, now with an average collision velocity of 4.84 km/sec and a $\langle P_i \rangle_{POP}$ of $2.72 \times 10^{-18}\,\mathrm{km}^{-2}\,\mathrm{year}^{-1}$.

III.A.2. 243 Ida. Asteroid 243 Ida intersects the orbits of 799 asteroids with $D > 30$ km, using the same main-belt population as for Gaspra. We find that the velocity distribution for Ida (Fig. 4) qualitatively resembles Gaspra's distribution, with a quasi-Gaussian shape and spiky fine structure. However, Ida's smaller eccentricity (0.042 compared with an eccentricity of 0.173 for Gaspra) yields lower collision velocities than Gaspra's. Furthermore, Ida's mean intrinsic collision probability for these 799 crossing asteroids is lower as well ($\langle P_i \rangle_{CROSS} = 5.04 \times 10^{-18}\,\mathrm{km}^{-2}\,\mathrm{year}^{-1}$). By normalizing the intrinsic collision probability to account for all main-belt asteroids, we find a substantially higher value than Gaspra's normalized value:

$$\langle P_i \rangle_{POP} = \langle P_i \rangle_{CROSS} \left(\frac{799}{1052} \right) = 3.83 \times 10^{-18}\,\mathrm{km}^{-2}\,\mathrm{year}^{-1}.$$

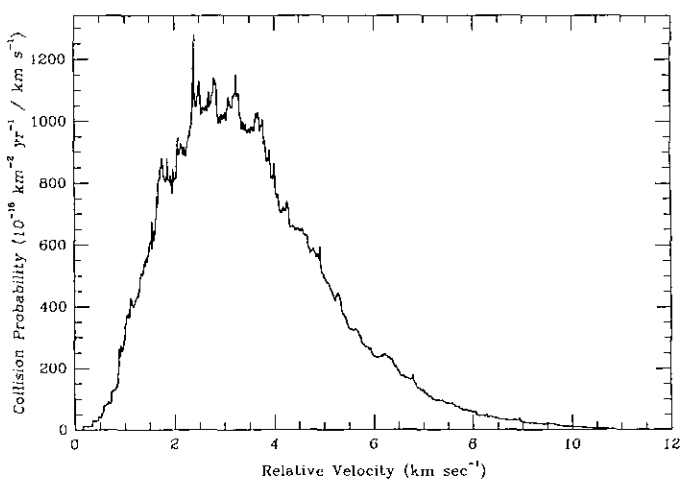

FIG. 4. Velocity distribution for the 799 main-belt asteroids of diameter >30 km (according to Minor Planet Center osculating elements) whose orbits intersect 243 Ida. The mean, median, and rms collision velocities are 3.55, 3.31 and 3.92 km/sec, respectively. The mean intrinsic collision probability of crossing bodies is: $\langle P_i \rangle_{CROSS} = 5.04 \times 10^{-18}$ km^{-2} year^{-1}.

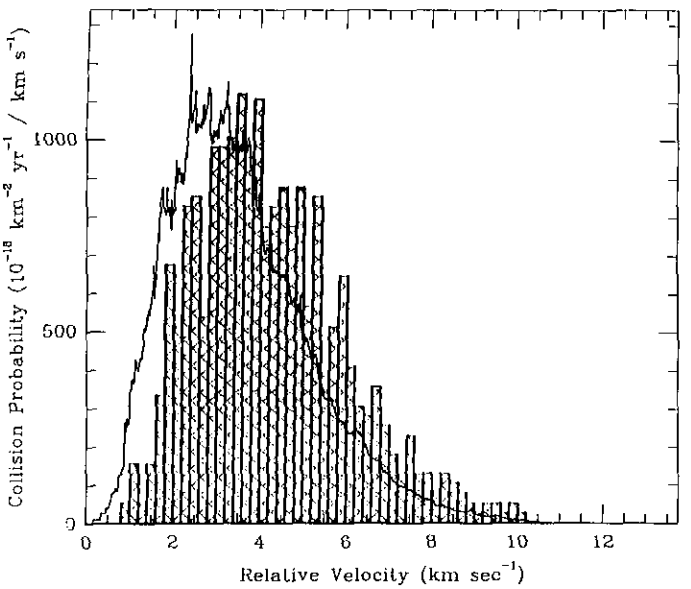

FIG. 5. Histogram of average velocities $\langle V \rangle$ for the same population in Fig. 4 superimposed on Fig. 4, from Binzel (1992). A comparison between this histogram and the velocity distribution from Fig. 4 shows that the histogram of average velocities misses some low collision velocities and some of the velocity structure present in the actual velocity distribution. Note that the reported mean velocity ($\langle V \rangle$ = 4.3 km/sec) for the histogram of average velocities is 0.4–1.0 km/sec away from the average velocities reported in Fig. 4. This inaccuracy is a consequence of the method of Namiki and Binzel (1991), who do not account for the relative probability of each possible collision geometry for each pair of asteroids.

Therefore, Ida is struck more often (~1.4 times) by the same population of main-belt asteroids as Gaspra. Moreover, since Ida is a Koronis family member, it is likely to be struck relatively often by other members of the Koronis family (Binzel 1988, 1992). Family members share similar orbital elements, which can result in high collision probabilities within that population of asteroids. However, typical impacts on Ida are at lower velocities than Gaspra, implying that a larger projectile is needed for catastrophic disruption. (For more information on velocity distributions for asteroid families, see Section III.D.) These two factors offset each other to some degree in calculation of Ida's collisional lifetime (see Section IV).

A comparison between our velocity distribution (from Fig. 4) and the histogram of average velocities for Ida (Binzel 1992) is shown in Fig. 5. Again we find striking differences between the distributions: (a) our distribution is shifted by more than 0.5 km/sec toward slower collisions, with our mean collision velocity ($\langle V \rangle$ = 3.55 km/sec) significantly less than Binzel's ($\langle V \rangle$ = 4.3 km/sec)), and (b) there is little correspondence between the fine structure found in our distribution and the artificial peaks and gaps of Binzel's distribution. These improvements could result in substantial changes to interpretations of the collisional history of Ida.

III.A.3. 2 Pallas. Not all velocity distributions for main-belt asteroids are the same; they can be significantly different from those seen in the Gaspra and Ida cases. One example is the velocity distribution for 2 Pallas, which is highly inclined and somewhat eccentric (a = 2.77, e = 0.235, i = 0.571 rad). Pallas intersects the orbits of 680 of the 682 asteroids with $D > 50$ km, using the same data set of osculating elements used by Farinella and Davis (1992).

The velocity distribution (Fig. 6) for this anomalous orbit is quite different from the more typical main-belt case: The distribution is more symmetrical, so the mean collision velocity occurs near the most probable velocities. The distribution shows little fine structure. The mean collision velocity for Pallas is also found to be much higher than typical main-belt bodies ($\langle V \rangle$ = 11.00 km/sec). These effects are a consequence of Pallas' high inclination, which, for most crossing pairs, increases encounter velocities and shifts the most probable velocities away from extreme values in the velocity distribution (i.e., in contrast to Fig. 1). The intrinsic collision probability for Pallas ($\langle P_i \rangle_{CROSS}$ = 2.13 × 10^{-18} km^{-2} year^{-1}), or equivalently,

$$\langle P_i \rangle_{POP} = \langle P_i \rangle_{CROSS} \left(\frac{680}{682} \right) = 2.13 \times 10^{-18}\,\mathrm{km}^{-2}\,\mathrm{year}^{-1},$$

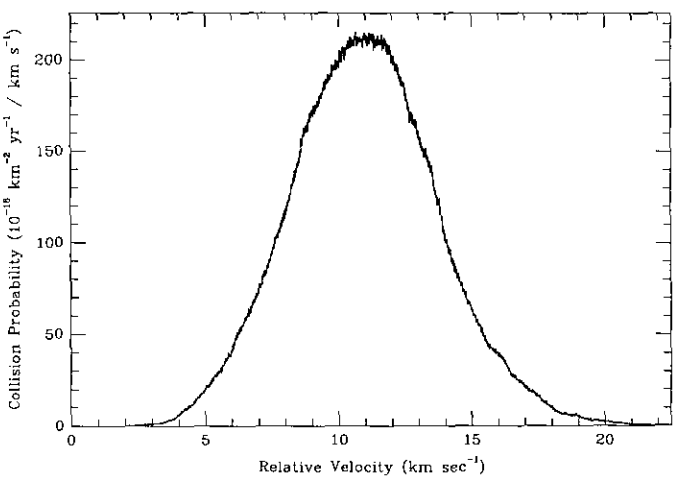

FIG. 6. Velocity distribution for the 680 main-belt asteroids of diameter >50 km whose orbits intersect 2 Pallas. The mean, median, and rms collision velocities are 11.00, 10.96, and 11.34 km/sec, respectively. The mean intrinsic collision probability of crossing bodies is: $\langle P_i \rangle_{CROSS}$ = 2.13 × 10^{-18} km^{-2} year^{-1}. Note that Pallas's velocity distribution shows higher probable collision velocities than most other distributions for main-belt asteroids, due to Pallas's high eccentricity and inclination. However, high velocities lower Pallas's overall collision probability per encounter.

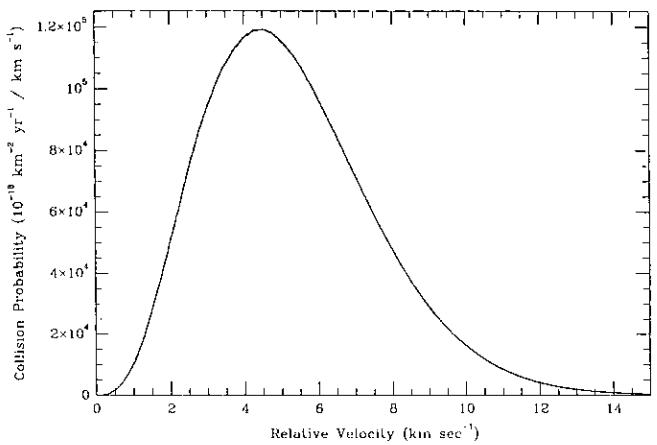

FIG. 7. Velocity distribution for the populations of all 682 main-belt asteroids ($D > 50$ km) impacting all other main-belt asteroids ($D > 50$ km). The distribution smooths out the spikiness of individual pairs, due to the large number of pairs that are added together. The mean, median, and mean collision velocities are 5.29, 5.03, and 5.79 km/sec, respectively. Note that the area under the curve, divided by the total number of possible colliding pairs, is the intrinsic collision probability for an average pair of intersecting asteroid orbits, $\langle P_i \rangle_{POP} = 2.86 \times 10^{-18}$ km^{-2} year^{-1}.

is unusually low for similar reasons; Pallas' high inclination keeps the asteroid away from most other main-belt asteroid throughout most of its orbit. Accordingly, the collisional evolution of Pallas may be significantly different from those of other main-belt asteroids similar in size.

III.B. Velocity Distributions for the Main Asteroid Belt

The velocity distribution for the main-belt was computed by summing the velocity distributions for all possible pairs among the 682 largest main-belt asteroids ($D >$ 50 km) (Fig. 7). We find it is qualitatively similar to Gaspra's (Fig. 2) or Ida's (Fig. 4). Again the high-velocity tail yields a mean collision velocity ($\langle V \rangle = 5.3$ km/sec) higher than the most probable collision velocity ($V \sim 4.4$ km/sec). This distribution is relatively smooth because large number of separate distributions for all pairs of asteroids (in this case $682 \times 681/2$) was summed to produce the curve.

Comparing our results with the histogram of average velocities by Farinella and Davis (1992) (Fig. 8), we find that the rather probable impacts at $V < 4$ km/sec are missed in their distribution. Their distribution also underestimates the probability of high-velocity collisions (>5.5 km/sec). The mean velocity ($\langle V \rangle = 5.3$ km/sec) for our results differs significantly from their values ($\langle V \rangle = 5.81$ km/sec). However, the average intrinsic collision probability reported by Farinella and Davis ($\langle P_i \rangle_{POP} = 2.85 \times 10^{-18}$ km^{-2} year^{-1}) is very close to our computed value ($\langle P_i \rangle_{POP} = 2.86 \times 10^{-18}$ km^{-2} year^{-1}).

III.C. Distributions of Velocity Direction Components

In the previous sections we showed distributions of the magnitude of impact velocities. We have used the same method to calculate the probability distribution for individual direction components of the collision velocity vector for the same set of 682 main-belt asteroids colliding among themselves. We calculate the velocity components for collisions relative to the invariable plane of the Solar System, with radial component V_R, azimuthal component V_θ, and normal-to-the invariant plane component V_Z. The distribution for these components is given in Fig. 9. Mean values are: $\langle V_R \rangle = 2.6$ km/sec, $\langle V_\theta \rangle = 0.88$ km/sec, and $\langle V_Z \rangle = 3.8$ km/sec; and root mean square velocities are: $\langle V_R^2 \rangle^{1/2} = 3.3$ km/sec, $\langle V_\theta^2 \rangle^{1/2} = 1.1$ km/sec, and $\langle V_Z^2 \rangle^{1/2} = 4.6$ km/sec.

The V_Z-component is significantly larger than the other two velocity components. We can quantify this anisotropy by considering the ratio between the mean square components in-plane and the mean square Z component as an isotropy index I. For an isotropic distribution,

$$I \equiv \frac{(\langle V_R^2 \rangle + \langle V_\theta^2 \rangle)/2}{\langle V_Z^2 \rangle} = 1.0. \quad (3)$$

In contrast, our rms velocities yield

$$I = \frac{(\langle V_R^2 \rangle + \langle V_\theta^2 \rangle)/2}{\langle V_Z^2 \rangle} = 0.29, \quad (4)$$

showing a substantial excess Z component.

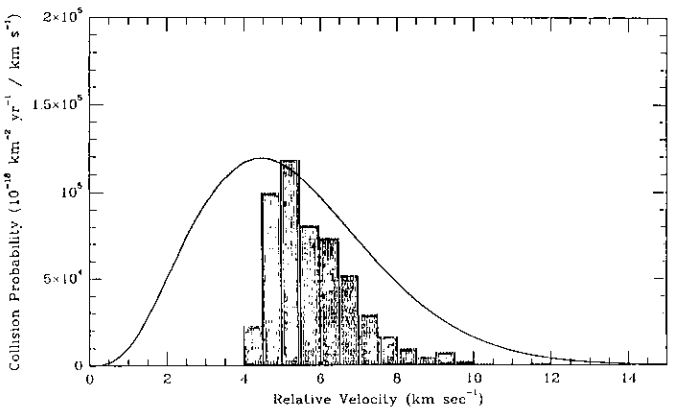

FIG. 8. Histogram of average velocities $\langle V \rangle$ for the same population in Fig. 7 superimposed on Fig. 7, from Farinella and Davis (1992). A comparison between this histogram and the velocity distribution from Fig. 7 shows that the histogram of average velocities misses both low and high collision velocities as well as most of the velocity structure present in the actual velocity distribution. Also, since Farinella and Davis do not account for the relative probability of each possible collision geometry, we find their average collision velocities are all nearly 0.3–0.5 km/sec higher than the actual values.

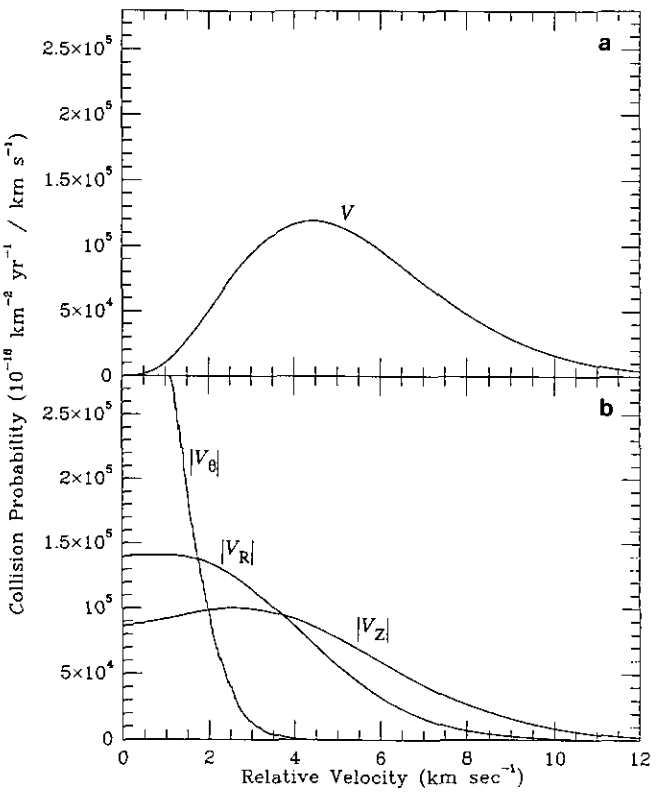

FIG. 9. Velocity component distributions relative to the invariable plane of the Solar System for the same population given in Fig. 7 (For Figs. 9–13: (a) total V; (b) radial component V_R, azimuthal component V_θ; and normal-to-the invariant plane component V_Z). The mean velocities for each component are: $\langle V_R \rangle$ = 2.6 km/sec; $\langle V_\theta \rangle$ = 0.9 km/sec; $\langle V_Z \rangle$ = 3.8 km/sec. Note that the area under each curve is equal. For the main-belt population, the most probable high collision velocities come from the Z direction.

These results are qualitatively similar to the tabulated "velocity dispersions" (σ_R, σ_θ, σ_Z) compound by Mikami and Ishida (1988) for nearly 2000 main-belt asteroids: σ_R = 2.4 km/sec, σ_θ = 1.2 km/sec, σ_Z = 3.2 km/sec. Mikami and Ishida used a relatively crude model to estimate impact velocities: They computed each asteroid's heliocentric velocity when it was closest to a heliocentric circle at the middle of the main-belt. It is unclear whether the "velocity dispersion" refers to mean values, rms values, or some other kind of average. If we assume it to be rms, the Mikami and Ishida results give

$$I \equiv \frac{(\langle \sigma_R^2 \rangle + \langle \sigma_\theta^2 \rangle)/2}{\langle \sigma_Z^2 \rangle} = 0.35. \quad (5)$$

Thus, our more accurate calculations show that the difference between mean Z-components and in-plane components is even greater than Mikami and Ishida found.

Magnusson (1993) computed the ratios of the mean-square components of the relative collision velocities using a method and population similar to those used by Farinella and Davis (1992), though he may have corrected problem I.1. He used components in an inertially fixed cartesian space, with Z (like ours) perpendicular to the invariable plane. He found the following velocity ratios: $\langle V_X^2 \rangle : \langle V_Y^2 \rangle : \langle V_Z^2 \rangle \approx 0.16 : 0.16 : 0.68$ (Magnusson's coordinate system requires that $\langle V_X^2 \rangle / \langle V_Y^2 \rangle = 1$, by definition). His values yield

$$I = \frac{(\langle V_X^2 \rangle + \langle V_Y^2 \rangle)/2}{\langle V_Z^2 \rangle} = 0.24. \quad (6)$$

Thus, our value of I lies midway between that of Magnusson and of Mikami and Ishida. All three confirm a substantial excess Z-component.

Magnusson (1993) suggested that the excess vertical velocity should concentrate asteroid spin axes near the ecliptic plane. However, since observations of asteroid rotation do not show such a concentration, Magnusson (1992) concluded that understanding of asteroid spin axis evolution is incomplete. Our complete velocity distribution may be a basis for further investigation of this issue.

III.D. Velocity Distributions for Asteroid Families

We have also computed the velocity distributions for the four most populous asteroid families in the main-belt (Zappalá *et al.*, 1990). These asteroid families are 15 Eunomia (71 members), 24 Themis (228), 158 Koronis (137), and 221 Eos (202). However, since very few of these asteroid family members have $D > 50$ km, it is probable that they do not provide a complete representative model for the orbits of the smaller asteroids of each family. Therefore, like Farinella and Davis (1992), we calculate the collision probabilities and velocities for the 30 lowest-numbered family members colliding with each other. We also use, as they do, osculating elements instead of proper elements to avoid the clustering of inclination for family members.

The velocity distribution for the Eos family is shown in Fig. 10. It is complex, non-Gaussian, and bimodal, with the spiky distributions of individual pairs emphasizing particular collision velocities. Much of this structure can be traced to the Eos family's orbital elements, which are tightly clustered. In particular, the inclinations of the Eos family members are all near 10°, producing certain highly probable collision geometries between individual pairs of asteroids. Since the most probable collisions occur near the apses, we expect the collision velocities associated with those orientations to be pronounced in the velocity distribution. As pairs of family members precess through a cycle, we find that two velocities for apsidal collisions dominate: (a) Low encounter velocities found when the

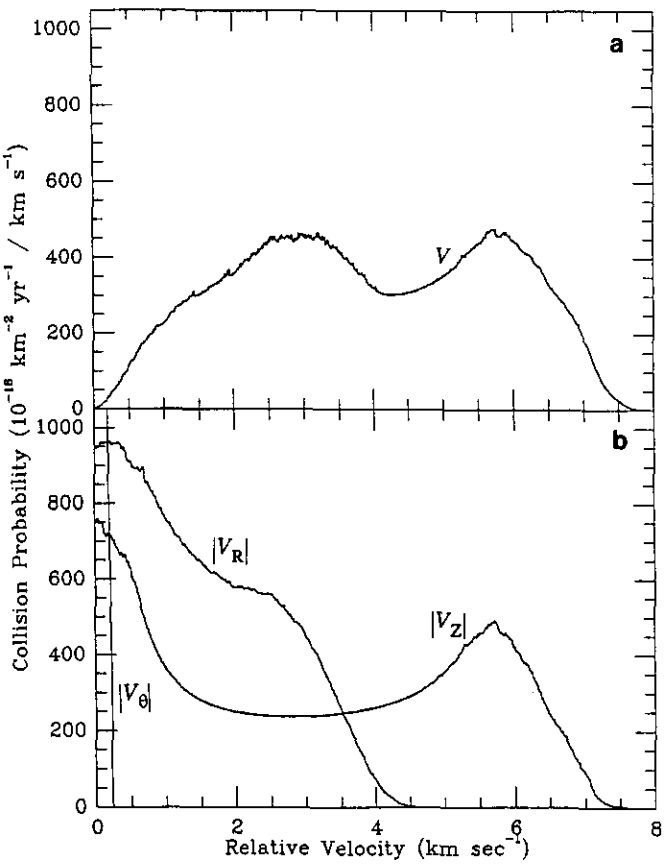

FIG. 10. Velocity component distributions for the 30 lowest numbered asteroids impacting each other (according to Minor Planet Center osculating elements) in the Eos asteroid family. The mean velocities for each component are $\langle V \rangle$ = 3.93 km/sec; $\langle V_R \rangle$ = 1.55 km/sec; $\langle V_\theta \rangle$ = 0.063 km/sec; $\langle V_Z \rangle$ = 3.23 km/sec, while the mean intrinsic collision probability is $\langle P_i \rangle_{POP} = 5.45 \times 10^{-18}$ km^{-2} year^{-1}. The double-lobed structure seen in the V_Z distribution dominates the other components, such that the overall velocity distribution is double-lobed. It results from the clustered inclinations of the Eos family members ($i \approx 10°$), which produces common collision geometries between individual pairs of asteroids.

pericenters are aligned and (b) high encounter velocities found when the pericenters are 180° out of phase. The double-lobed structure in the V_Z distribution shows which collision velocities correspond to these most likely collision geometries. In fact, the V_Z distribution's shape is wide enough that it dominates the structure of the other components, creating the double-humped structure for the velocity magnitude (V) distribution.

Next we consider the velocity distribution for the Themis family, which is double-humped and complex as well (Fig. 11). However, the Themis distribution's structure was not produced in the same way as the Eos distribution's structure. In this case, the inclinations for Themis family members were so low ($i \approx 1°$–$2°$) that precession of the nodes produced little structure in the V_Z distribution. However, since the eccentricities of the Themis family members are nearly all between ~0.1 and 0.2, precession of the apsides should produce both low and high collision velocities near the apses of each family member's orbit, where collisions are more probable (e.g., near 1 and 5 km/sec). By summing the distributions for all Themis members, we find that these velocities are most likely in the V_R distribution, such that a double-lobed structure is produced there. This feature dominates the structure of the velocity distribution, because the other components' are dominated by low velocities.

Other families produce even more complex velocity distributions. The Eunomia family's velocity distribution shows evidence for multiple lobes, with a peak near V = 6 km/sec (Fig. 12). This structure reflects a clustering of

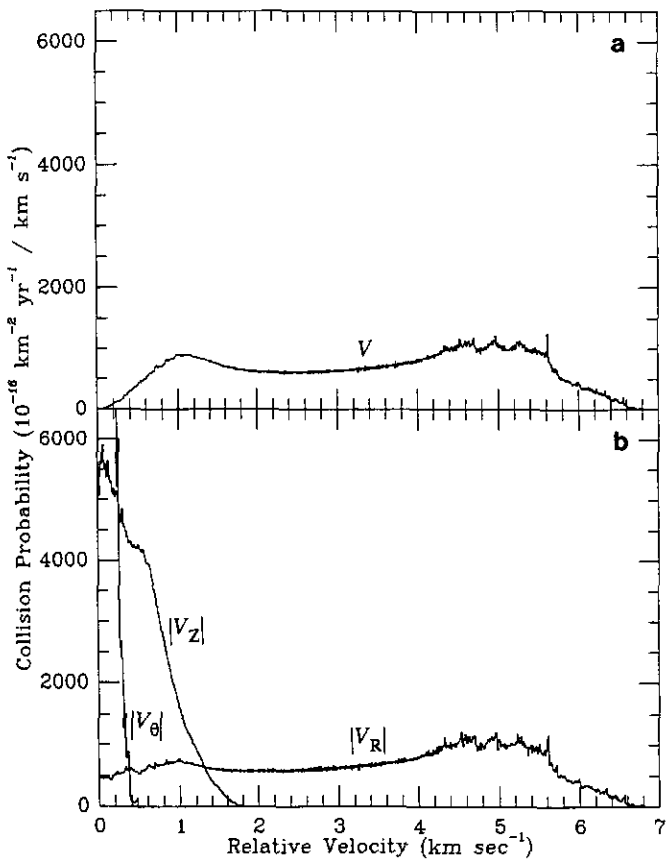

FIG. 11. Velocity component distributions for the 30 lowest numbered asteroids impacting each other (according to Minor Planet Center osculating elements) in the Themis asteroid family. The mean velocities for each component are: $\langle V \rangle$ = 3.46 km/sec; $\langle V_R \rangle$ = 3.36 km/sec; $\langle V_\theta \rangle$ = 0.11 km/sec; $\langle V_Z \rangle$ = 0.50 km/sec, while the mean intrinsic collision probability is $\langle P_i \rangle_{POP} = 10.1 \times 10^{-18}$ km^{-2} year^{-1}. The double-lobed structure seen in the V_R distribution dominates the other components, such that the overall velocity distribution is double-lobed. In this case, the clustered inclinations are too small to produce the effect seen in Fig. 10. However, the clustered eccentricities of Themis family members (between e ~ 0.1 and 0.2), produces a similar effect.

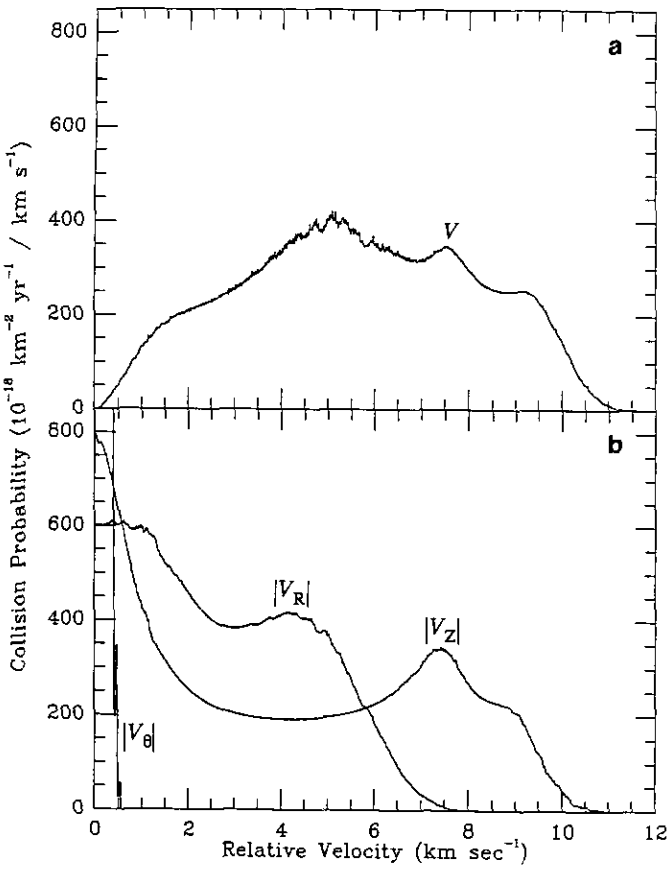

FIG. 12. Velocity component distributions for the 30 lowest number asteroids impacting each other (according to Minor Planet Center osculating elements) in the Eunomia asteroid family. The mean velocities for each component are: $\langle V \rangle$ = 5.62 km/sec; $\langle V_R \rangle$ = 2.76 km/sec; $\langle V_\theta \rangle$ = 0.12 km/sec; $\langle V_Z \rangle$ = 4.17 km/sec, while the mean intrinsic collision probability is $\langle P_i \rangle_{POP} = 6.25 \times 10^{-18}$ km^{-2} year^{-1}. In this case, clustering over high inclinations ($i \sim 13°$) and eccentricities ($e \sim 0.1$–0.2), produce double-lobed structure in both the V_R and the V_Z distributions. The resultant distribution is complex and multihumped.

high inclinations ($i \approx 13°$) and eccentricities ($e \approx 0.1$–0.2), which combine the effects seen in the Eos and Themis families, respectively. Since each of these orbital element groupings produce the double-lobed structure seen in the V_R and V_Z distributions, the combination of both components produces a complex velocity distribution which cannot be represented by any single velocity.

The velocity distribution for the Koronis family is qualitatively more Gaussian and less complex than the other families discussed (Fig. 13). The inclination for most Koronis family members is near 2°, minimizing the structure seen in the V_Z distribution. Also, the eccentricities are low, minimizing the collision probabilities of the apses positions which produce double-lobed structure in the V_R distribution. Moreover, these low eccentricities and inclinations yield low collision velocities between family members, where the most probable collision velocities are quite low (the mean, median, and rms velocities are all near 1.5 km/sec).

The average intrinsic collision probabilities ($\langle P_i \rangle_{POP}$) for the Eos, Themis, Eunomia, and Koronis families members (with themselves) are 5.45, 10.12, 6.25, and 13.75 km^{-2} year^{-1}, respectively, all higher than the average collision probability between main-belt asteroids of 2.86×10^{-18} km^{-2} year^{-1}. Thus, collisions between members of the same family are 2 to 5 times more likely than collisions between other main-belt asteroids, at least as great as the factor of 2 to 3 found by Farinella and Davis.

Furthermore, the velocity distributions show that the most probable collision velocities are lower for encounters among family members than with nonfamily members. However, the velocity distributions for each family show irregular structure, implying that the clustering of orbital elements for family members can produce pre-

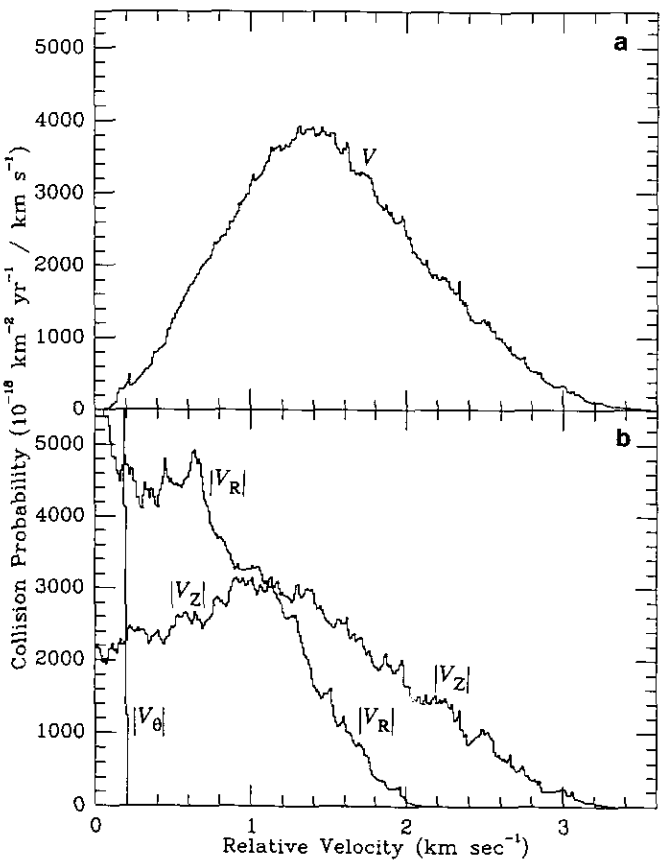

FIG. 13. Velocity component distributions for the 30 lowest numbered asteroids impacting each other (according to Minor Planet Center osculating elements) in the Koronis asteroid family. The mean velocities for each component are: $\langle V \rangle$ = 1.51 km/sec; $\langle V_R \rangle$ = 1.21 km/sec; $\langle V_\theta \rangle$ = 0.069 km/sec; $\langle V_Z \rangle$ = 6.9 km/sec, while the mean intrinsic collision probability is $\langle P_i \rangle_{POP} = 13.8 \times 10^{-18}$ km^{-2} year^{-1}. In this case, the clustered inclinations are too small ($i \approx 1°$) to produce a significant double-lobed effect. The resulting overall distribution is more Gaussian than other family's distributions.

ferred collision geometries between individual pairs of asteroids. These preferred geometries are much more pronounced than more typical collision geometries between main-belt asteroids. Consequently, velocity distributions for asteroid families are very different from those calculated for asteroids in the main-belt.

Binzel (1988) suggested that low collision velocities may be more effective in changing asteroid spin rates than high velocities, since the target is less likely to disrupt. Therefore, he reasoned, the rotation rates of the Koronis and Eos families may be dominated by intrafamily collisions, which have lower collision velocities than typical nonfamily asteroids. However, we have seen that low-velocity collisions between main-belt asteroids also occur frequently. In fact, the number of collisions between asteroid family members may be small compared to the number of low-velocity collisions from other main-belt asteroids. Although individual collisions of a given family member with another family member are more probable than with a main-belt asteroid, there are far more of the latter (even at lower velocities), so intrafamily collisions do not dominate impacts into family members. It remains possible that intrafamily collisions dominate at smaller asteroid sizes (Cellino *et al.* 1991), but we currently lack information needed to resolve this issue.

IV. EFFECTS OF VELOCITY DISTRIBUTIONS ON ASTEROID DISRUPTION RATES

Most velocity distributions in the main-belt show similar characteristics: a long, high-velocity tail and high probability of encounters at lower-than-average velocities. For issues relating to asteroid lifetime and catastrophic disruption, these features are potentially significant. Since high-velocity impacts among asteroids occur with substantial frequency, smaller asteroids can disrupt larger bodies than previously assumed by models of asteroidal collisional evolution. Thus, a population dominated by small bodies (e.g., as suggested by the Galileo imaging of Gaspra (Belton *et al.* 1992)) could undergo frequent disruptions of the larger bodies, as many small bodies strike at high velocities. On the other hand, the most probable impact velocities are lower than the mean. These two effects offset one another to some degree.

In order to compute the disruption lifetime of an asteroid in the main-belt, we require three elements:

1. Criteria for disruption as a function of (a) target size, strength, and mass; (b) impactor size and mass; and (c) the relative collision velocity.

2. The number of bodies in the impacting population as a function of size.

3. The probability distribution for collision velocities between a target asteroid and an impacting population as computed in this paper (and previously generally assumed to be a single velocity).

TABLE I
Summary of Disruption Rates for Selected Targets in Section IV (Units 10^{-11} year^{-1})

	200-km Main-Belt target	Gaspra	Ida
From previous literature	2.77	195	133
Corrected to our $\langle V \rangle$ and $\langle P_i \rangle_{POP}$	2.65	167	37.8[a]
+ Corrected for our cross-section	3.88	176	44.0[a]
+ Corrected for velocity distribution	3.82	181	44.1[a]

[a] Different disruption criteria than previous literature.

In this section, we combine various estimates of (1) and (2) with our results for the velocity distributions (3) to calculate the frequency of catastrophic disruption for a given main-belt target. In each of these illustrative cases, in order to compare with calculations by previous workers, we adopt their models of (1) and (2) and then consider the effect of replacing their average (or estimated) velocity values with our velocity distributions. It should be recognized that some of the models for (1) and (2) are controversial and subject to revision, but here we adopt the same models as previous authors for the specific purpose of quantifying the importance of (3). The results of the following examples are summarized in Table I.

IV.A. 951 Gaspra

Based on the cratering record observed on Gaspra by the Galileo spacecraft, Belton *et al.* estimated the size-frequency distribution of the main-belt asteroids hitting Gaspra to be a power law with incremental index of -2.95 from the small asteroids of the Palomar–Leiden survey (Van Houten *et al.* 1970) down to asteroids of 175 m diameter, steepening to an index of -3.5 for smaller asteroids.

Belton *et al.* adopted the disruption model of Farinella *et al.* (1991), which is based on disruption criteria used by Greenberg *et al.* (1978): Half the impact kinetic energy, divided by the target volume must exceed the target's impact strength, or equivalently

$$\frac{D_P}{D_T} = \left(\frac{4S}{\rho V^2}\right)^{1/3}, \tag{7}$$

where ρ is the material density (2.5 g cm^{-3}), D_P and D_T are the projectile and target diameters, respectively, and S is the impact strength. Impact strength is defined as the energy density needed to produce a barely catastrophic impact (50% of the target mass leaving at escape velocity).

Values adopted for ρ, D_T, and S were taken to be 2.5 g cm^{-3}, 16 km, and 2×10^6 erg cm^{-3}, respectively. A mean value for the impact velocity of 5.45 km/sec was found by Farinella *et al.* (presumably using the algorithm of Farinella and Davis, 1991), as well as $\langle P_i \rangle_{POP} = 2.7 \times 10^{-18}$ km^{-2} year^{-1}. These parameters yielded a minimum disruption projectile size of 350 m.

With that disruption model and projectile size distribution, Belton *et al.*, inferred an impact frequency of disruptors of 2×10^{-9} year^{-1}, or a mean lifetime of 500 Myr. More precisely, using their parameters, we obtain a rate of 1.95×10^{-9} year^{-1}. We note that several aspects of this procedure are questionable. For example, Greenberg *et al.* (1993) have shown that both the asteroid size distribution and the disruption criteria likely need revision. However, for purposes of this study, we restrict our considerations to the effect of correcting the impact velocity distribution.

When we replace the Belton *et al.* mean collision velocity and $\langle P_i \rangle_{POP}$ values with our results from Section III.A (4.84 km/sec and 2.72×10^{-18} km^{-2} year^{-1}, respectively), we obtain a minimum disruptor diameter of 383 m and a disruption rate of 1.67×10^{-9} year^{-1}, a correction of -14%. In this calculation as well as that of Farinella and Davis, the collision cross section is assumed to be that of the target, because most disruptors are much smaller than the target. However, some potential disruptors may be comparable in size to Gaspra. If we use the cross section for both the impactor and the projectile over the full range of sizes of disruptors, we obtain a disruption rate of 1.76×10^{-9} year^{-1}. Finally, if we use the actual velocity distribution that we calculated for Gaspra crossers with $D > 50$ km (the same population considered by Farinella and Davis (1992)), there is a substantial probability of disruption by impactors smaller than 250 m, but the disruption rate changes by only 3% to 1.81×10^{-9} year^{-1}. Thus the greatest correction is due to using the correct average collision velocity and $\langle P_i \rangle_{POP}$, while further corrections such as the complete velocity distribution are somewhat smaller.

Greenberg *et al.* (1993) introduced a disruption model based on hydrocode simulations, which showed Gaspra to be more resistant to disruption than indicated by strength-scaled models like that used by Farinella *et al.* (1991). The disruption lifetime was found to be twice that found by Farinella *et al.* However, again we find that using the full velocity distribution gives corrections <10%.

IV.B. A Large Main-Belt Target

Farinella and Davis (1992) considered a hypothetical 200- to 250-km main-belt asteroid as a target. They adopted a disruption model that is controlled by the gravity of this large asteroid. Davis *et al.* (1989) showed that the criterion for disruption in such a case may take the same form as (7), where the parameter S now represents a combination of parameters that describe the input efficiency of kinetic energy and the velocity distribution of debris. With their mean collision velocity of 5.81 km/sec and $\langle P_i \rangle_{POP} = 2.85 \times 10^{-18}$ km^{-2} year^{-1}, they found a minimum disruptor diameter of 50 km and (using known numbers of asteroids in that size range and an effective strength of $\sim 10^9$ erg cm^{-3}) a frequency of disrupting impacts of 3.0×10^{-11} year^{-1}.

Evidently these values were approximations, because a precise value of the target body's diameter was not specified. If we try to reproduce their calculation for a 200-km target, using all the same parameters as they did, we obtain a disruptor diameter of 54 km and disruption frequency of 2.77×10^{-11} year^{-1}. When we replace their mean collision velocity and $\langle P_i \rangle_{POP}$ values with our results from Section III.B (5.29 km/sec and 2.86×10^{-18} km^{-2} year^{-1}, respectively), we obtain a minimum disruptor diameter of 58 km and a disruption rate of 2.65×10^{-11} year^{-1}, a very small correction.

However, for comparison with Farinella and Davis, the above results assume that the collision cross section equals the target's cross section. If we take into account the cross section of the larger disruptors, the disruption rate becomes 3.88×10^{-11} year^{-1}, a substantial correction. If we use our calculated velocity distribution (Fig. 7), there is some probability of disruption by impactors as small as 20 km, but the disruption rate only changes slightly to 3.82×10^{-11} year^{-1}. In the case of the main-belt population, correcting the velocity distribution is numerically less important than properly accounting for the collision cross section.

IV.C. 243 Ida

Ida's collisional lifetime was calculated by Binzel (1992) to be 750 Myr, based on a strength-scaling disruption law, his values for mean velocity and collision probability (see Section III.A), an assumed size-frequency distribution for asteroids in the main-belt, and Ida's material strength.

However, Nolan *et al.* (1992, see also Greenberg *et al.* 1993) found that small asteroids are much more resistant to disruption than predicted by strength scaling. In fact, for Gaspra, they found that disruption occurs when the crater diameter predicted by gravity scaling is comparable to the target diameter. Here we assume that the same relationship holds for Ida. According to Schmidt–Holsapple scaling (in Melosh 1989), the gravity-scaling size law for a transient crater (before slumping) D_{AT} is

$$D_{AT} = 1.8 \rho_P^{0.11} \rho_T^{-1/3} g^{-0.22} D_P^{0.13} W^{0.22}, \quad (8)$$

where D_P and ρ_P are the projectile's diameter and density, respectively, g and ρ_T are the target's gravity and density,

respectively, and W is the projectile's explosive energy (yield). We substitute Ida's mean diameter (30 km) for the crater diameter and use density 2.7 g cm^{-3}, the Belton *et al.* adopted size distribution for small bodies, and our mean collision velocity and $\langle P_i \rangle_{POP}$ from Section III.A, yielding a minimum disruptor diameter of about 2 km and a lifetime of 2.64 Gyr (disruption frequency of 3.78×10^{-10} year^{-1}). Thus, these parameters yield a lifetime nearly 3.5 times as long as estimated by Binzel.

When we properly account for the collisional cross section, the lifetime becomes 2.27 Gyr (disruption frequency of 4.40×10^{-10} year^{-1}), a 14% change. When we use the velocity distribution of Fig. 4, rather than its mean value, the lifetime is unchanged. As in the case of the typical 200-km main-belt body, the incorporation of the correct cross section for larger disruptions is the most important factor. We also note that the Ida lifetime may be different than calculated here if its membership in the Koronis family means that it is impacted by a different size distribution than we have assumed here.

V. CONCLUSIONS

In this paper, we have investigated the distributions of collision velocities among asteroids. We have shown that collisions in the main-belt occur over a wide and asymmetric range of velocities which must be taken into account to model accurately the collisional lifetimes of asteroids. By applying these velocities to other effects of asteroid collisional evolution, we can obtain a much broader understanding of the relationship between collision velocities and physical processes such as asteroid spin evolution, ejecta removal, regolith formation, and disruption events.

We have calculated velocity distributions for collisions of single asteroids, including Gaspra, Ida, and Pallas, with the main-belt. By combining all of the individual velocity distributions of pairs in the main-belt, we obtained a velocity distribution for the main-belt population. We find that summing large number of individual distributions smooths any spikiness in the main-belt distribution. There is a significant probability of impacts at velocities greater than 10 km/sec. The velocity component distributions for the main-belt show that high collision velocities are most likely in the direction normal to the invariant plane of the Solar System. The implications of these collision orientations are not clear, but they may affect asteroid spin axis and spin rate evolution. More work in this area is clearly needed.

The velocity distributions for collisions within asteroid families show relatively high collision probabilities and low collision velocities. However, the distributions also show irregular structure, where the clustering of orbital elements often produces favored collision geometries and velocities. These favored velocities may affect the collisional evolution of individual family members, though it is not clear if the signal from interfamily collisions can be detected through the more prominent, higher-velocity collisions from other asteroids in the main-belt. The *in situ* investigation of Koronis family member 243 Ida by Galielo may prove enlightening.

We have also computed collisional lifetimes for various asteroids in the main-belt. Asteroid disruption lifetimes depend strongly on model assumptions regarding collision velocities, disruption scaling laws, and the size distribution of the impactor population. For example, disruption lifetimes may vary significantly depending on what disruption scaling relationships are adopted. Specifically, in the cases of Gaspra and Ida, numerical hydrocode models and corresponding modification of the gravity-scaling law of Schmidt–Holsapple (Melosh 1989) produces significantly longer disruption lifetimes than strength-scaling laws. In general, the importance of using a full velocity distribution will vary depending on the particular shape of the distribution and on the disruption criteria and projectile size distribution.

However, we find that average collision velocities, as long as the latter are correct averages, yield results similar to those obtained with complete velocity distributions. Velocity distributions do tend to change collisional lifetimes a bit, relative to lifetimes computed from average velocities. It is also very important to correctly account for the collision cross section over the full range of sizes of disruptors in the impacting population.

Applications for velocity distributions exist in many regions of asteroid collisional evolution studies. For example, asteroid rotation rates and spin axis orientations depend on many factors: collision orientation, impact velocity, and the size and composition of both the projectile and target bodies. Since many of these components are modeled in generating velocity distributions and collisional lifetimes, we should be able to modify our existing programs to investigate these processes.

Our understanding of asteroid collisional processes, such as collisional disruption, ejecta removal, and regolith formation, is currently undergoing a revolution due to rapid advances in many areas. The advent of numerical hydrocodes now allows us to model complicated physical processes occurring during collision events, which enhances our perception of laboratory results and the cratering record on various bodies. In addition, our knowledge about the size, number, and distribution of asteroid in the Solar System continues to increase. Now, with our development of velocity distributions, we can model the collision evolution of particular asteroids more accurately than ever before. Though many questions need to be resolved, we continue to make

progress in understanding the nature of asteroids and their evolution.

ACKNOWLEDGMENTS

We thank David Tholen, Don Davis, and Paolo Farinella for providing us with machine-readable files of the orbital elements necessary for the calculations presented in this paper. We also thank Nori Namiki, Rick Binzel, Paolo Farinella, and Shigeru Ida for their helpful discussions, comments, insights, and reviews. This work was supported by Grant NAGW-1029 from NASA's Planetary Geology and Geophysics Program.

REFERENCES

ARNOLD, J. R. 1965. The origin of meteorites as small bodies. II. The model. *Astrophys. J.* **141,** 1536–1547.

ASPHAUG, E., AND H. J. MELOSH 1993. The Stickney impact of Phobos: A dynamical model. *Icarus* **101,** 144–164.

BELTON, M. J. S., *et al.* 1992. Galileo encounter with 951 Gaspra: First pictures of an asteroid. *Science* **257,** 1647.

BINZEL, R. P. 1988. Collisional evolution in the Eos and Koronis asteroid families: Observational and numerical results. *Icarus* **73,** 303–313.

BINZEL, R. P. 1992. 1991 Urey prize lecture: Physical evolution in the Solar System–Present observations as a key to the past. *Icarus* **100,** 274–287.

BOTTKE, W. F., AND R. GREENBERG 1993. Asteroidal collision probabilities. *Geophys. Res. Lett.* **20,** 879–881.

CELLINO, A., V. ZAPPALÁ, AND P. FARINELLA 1991. The size distribution of main-belt asteroids from IRAS data. *Mon. Not. R. Astr. Soc.* **25,** 561–574.

DAVIS, D. R., P. FARINELLA, P. PAOLICCHI, S. J. WEIDENSCHILLING, AND R. P. BINZEL 1989. Asteroid collisional history: Effects on sizes and spins. In *Asteroids II* (R. P. Binzel, T. Gehrels, and M. S. Matthews, Eds.), pp. 805–826. Univ. of Arizona Press, Tucson.

DAVIS, D. R., P. FARINELLA, AND M. CARPINO 1992. Asteroid collisional frequencies: Variations in space and time. *Lunar Planet. Sci. XXIII,* 283–284.

FARINELLA, P., D. R. DAVIS, A. CELLINO, AND V. ZAPPALÁ 1991. The collision lifetime of 951 Gaspra. *Lunar Planet. Sci. XXII,* 363–364. (Also in an unpublished preprint)

FARINELLA, P., AND D. R. DAVIS 1992. Collision rates and impact velocities in the Main Asteroid Belt. *Icarus* **97,** 111–123.

GREENBERG, R. 1982. Orbital interactions: A new geometrical formalism. *Astron. J.* **87,** 184–195.

GREENBERG, R., M. C. NOLAN, W. F. BOTTKE, AND R. A. KOLVOORD 1993. Collisional history of Gaspra. Submitted for publication.

HOUSEN, K. R., AND K. A. HOLSAPPLE 1990. On the fragmentation of asteroids and planetary satellites. *Icarus* **84,** 226–253.

KNEZEVIC, A., A. MILANI, P. FARINELLA, CH. FROESCHLE, AND CL. FROESCHLE 1991. Secular resonances from 2 to 50 AU. *Icarus* **93,** 316–330.

MAGNUSSON, P. 1993. The distribution of collision velocities in the asteroid belt. Submitted for publication.

MAGNUSSON, P. 1992. Spin vectors of asteroids: Determination and cosmological significance. Invited paper submitted for inclusion in the *Proceedings of the 1992 Liége International Astrophysical Colloquium: Observations and Physical Properties of Small Solar System Bodies* (J. Surdej, Eds.) Belgium.

MELOSH, H. J. 1989. *Impact Cratering: A Geologic Process.* Oxford Univ. Press, New York.

MIKAMI, T., AND K. ISHIDA 1988. Kinematic structure of the asteroid belt. *Publ. Astron. Soc. Japan* **40,** 627–636.

MILANI, A., AND Z. KNEZEVIC 1990. Secular perturbation theory and computation of asteroid proper elements. *Celest. Mech.* **49,** 247–411.

NAMIKI, N., AND R. P. BINZEL 1991. "951 Gaspra: A pre-Galileo estimate of its surface evolution. *Geophys. Res. Lett.* **18,** 1155–1158.

NOLAN, M. C., E. ASPHAUG, AND R. GREENBERG 1992. Numerical simulation of impacts on small asteroids *Bull. Am. Astron. Soc.* **24,** 959–960.

ÖPIK, E. J. 1951. Collisional probabilities with the planets and the distribution of interplanetary matter. *Proc. R. Irish Acad.* **A54,** 165–199. (See also Öpik 1976, *Interplanetary Encounters,* Elsevier.)

PRESS, W. H., B. P. FLANNERY, S. A. TEUKOLSKY, AND W. T. VETTERLING 1986. *Numerical Recipes.* Cambridge Univ. Press.

VAN HOUTEN, C. J., I. VAN HOUTEN-GROENVELD, P. HERGET, T. GEHRELS 1970. The Palomar–Leiden Survey of faint minor planets. *Astron. Astrophys. Suppl.* **2,** 339–448.

WETHERILL, G. W. 1967. Collisions in the asteroid belt. *J. Geophys. Res.* **72,** 2429–2444.

ZAPPALÁ, V., A. CELLINO, P. FARINELLA, AND Z. KNEZEVIC 1990. Asteroid families. I. Identification by hierarchical clustering and reliability assessment. *Astron. J.* **100,** 2030–2046.